Scientia Agricola
http://dx.doi.org/10.1590/0103-9016-2014-0142

Field-scale spatial correlation between contents of iron oxides and CO_2 emission in an Oxisol cultivated with sugarcane

Angélica Santos Rabelo de Souza Bahia[1], José Marques Júnior[1]*, Alan Rodrigo Panosso[2], Livia Arantes Camargo[1], Diego Silva Siqueira[1], Daniel De Bortoli Teixeira[1], Newton La Scala Júnior[1]

[1]São Paulo State University/FCAV, Via de Acesso Prof. Paulo Donato Castellane s/n – 14883-292 – Jaboticabal, SP – Brazil.
[2]São Paulo State University/FEIS, Av. Brasil 56 – 15385-000 – Ilha Solteira, SP – Brazil.
*Corresponding author <marques@fcav.unesp.br>

Edited by: Clyde William Fraisse / Carlos Eduardo Pellegrino Cerri

Received May 14, 2013
Accepted May 21, 2014

ABSTRACT:Soil CO_2 emission (FCO_2) is one of the main sources of carbon release into the atmosphere. Moreover, FCO_2 is related to soil attributes governing the transfer of gases from soil to the atmosphere. This study aimed firstly to describe the spatial variability of hematite (Hm), goethite (Gt), iron extracted with sodium dithionite-citrate-bicarbonate (Fe_d) contents, soil CO_2 emission (FCO_2) and free-water porosity (FWP) and secondly, to develop statistical models to predict the above mentioned factors in an Oxisol cultivated under manual harvesting of sugarcane (*Saccharum* spp.) in southeastern Brazil. The study was conducted on an irregular 50 m × 50 m grid containing 89 points, each 0.5-10 m apart. The 0-0.1 m soil layer at each sampling point was used to assess soil FCO_2, moisture and total pore volume. The results were subjected to descriptive statistical and geostatistical analyses using auto- and cross-semivariograms. All soil attributes exhibited a spatial dependence structure and the experimental semivariograms fitted spherical and exponential models. The Gt content was the individual attribute that exhibited the highest linear and spatial correlation, especially with FCO_2. We were able to use diffuse reflectance spectroscopy to map large areas, which allows for easy identification and estimation of soil attributes such as FCO_2 and FWP. Geostatistical techniques faciltate the interpretation of spatial relationships between soil respiration and the examined properties.
Keywords: hematite, goethite, soil respiration, geostatistics, cross-semivariograms

Introduction

Soil CO_2 emission (FCO_2) is a reliable indicator of global climate change as it is one of the major sources of carbon loss from soil (Cerri et al., 2009). FCO_2 is related to a number of attributes that govern the release of gas into the atmosphere such as soil porosity (Panosso et al., 2012), temperature, moisture (Panosso et al., 2009), and mineralogical composition (La Scala et al., 2000). These attributes are closely related to soil aggregation (Cañasveras et al., 2010), which in turn is directly associated with soil gas emission.

Iron oxides are widely used as pedoenvironmental indicators on the grounds of their sensitivity to the specific conditions of soil formation processes (Schwertmann and Taylor, 1989). These minerals influence the physical and chemical behavior of tropical and subtropical soils through changes in their dynamics, a phenomenon which testifies to their high significance (Cornell and Schwertmann, 2003). For example, sugarcane (*Saccharum* spp.) management of crop residues (cane) can alter several factors such as soil moisture and the concentration of organic ligands, which are involved in the chemical reduction and chelation of iron oxides (Inda et al., 2013). This further confirms the relationship between iron minerals and CO_2 via its production or release from soil.

Diffuse reflectance spectroscopy (DRS) has been widely used to identify and quantify iron oxides in soils and sediments (Torrent and Barrón, 2008; Viscarra Rossel and Webster, 2011), examine the effects of organic matter thereupon (Demattê et al., 2006) and estimate aggregate stability (Cañasveras et al., 2010). The spectral behavior of soils depends on their physical, chemical and biological properties. Warrick and Nielsen (1980), Cambardella et al. (1994), Camargo et al. (2008; 2014) reported a high spatial variability in soil attributes, including FCO_2 (Panosso et al., 2012) and mineralogical composition (Bahia et al., 2014).

Geostatistics is a powerful auxiliary mapping tool which, however, is often disregarded in cases of more intensive sampling requirements. Thus, the DRS technique provides an effective choice for this task, since it allows for easy identification and estimation of soil attributes. In this context, this study aimed : i) to describe the spatial variability of the hematite, goethite, iron extracted with sodium dithionite-citrate-bicarbonate, soil CO_2 emission and free water porosity; and ii) to develop statistical models to predict the above mentioned factors in an Oxisol cultivated under manual harvesting of sugarcane in southeastern Brazil.

Materials and Methods

Study area

The study was conducted in Guariba, in the state of São Paulo, Brazil (21°24 S; 48°09′ W; 550 m above sea level). The climate is of the B_2rB'4a', mesothermal type according to the Thornthwaite classification system, with rainy summers and dry winters. Average annual precipitation is about 1,425 mm mainly concentrated in the Oct to Mar period. Average annual temperature for

the last 30 years has been 22.2 °C and we used a clayey Typic Eutrudox (Soil Survey Staff, 1999) on a 3 % slope. The area had been cropped with sugarcane for the previous 38 years, the last eight with mechanical green-harvested (not-burned). The cropping residues left in the soil are estimated to amount to 12 t ha^{-1} each year. The study was conducted on a 50 m × 50 m irregular sampling grid containing 89 variably spaced points 0.5-10 m apart (Figure 1).

Field and laboratory analysis

Soil CO_2 emission (FCO_2) was measured with two portable LI-8100 automated soil CO_2 flux system (La Scala et al., 2000). The LI-8100 uses infrared spectroscopic measurements to monitor changes in CO_2 concentration inside a closed chamber. The chamber is a closed system with an internal volume of 854.2 cm^3 and a circular soil contact area of 83.7 cm^2. It was coupled to a PVC collar that had been previously installed at every 89-sample points. Measurements were taken in the morning and afternoon at every sampling point over a period of six days to calculate an average FCO_2 value. Soil temperature (T_s) was monitored at the same time/simultaneously by using the thermistor-based 0.20 m probe included in the LI-8100. The probe was inserted 5 cm into the soil near the PCV collar. Soil moisture (M_s) was recorded with a portable hydrosensing system consisting of a TDR probe.

FCO_2, T_s and M_s measurements were followed by a sampling of the 0.0-0.1 m soil layer at the 89 points on the grid. Samples were allowed to dry in the air, ground and screened through a 2 mm mesh prior to routine analysis. Soil density (D_s) was determined in samples collected with a cylinder sampler providing specimens 0.04 m high and 0.05 m in diameter. Total pore volume (TPV) was calculated from density measurements and pore distribution by using a funnel furnished with a porous plate loaded with pre-soaked samples and placed under a 0.6 m high water column. Free water porosity (FWP) was calculated as the difference between total pore volume (TPV) and the pore fraction filled by water, which was equivalent to M_s. These soil attributes were determined as in Panosso et al. (2012).

The determination of iron content in the total of pedogenic iron oxides extracted by sodium dithionite-citrate-bicarbonate (Fe_d) followed the methodology of Mehra and Jackson (1960) and the levels of iron extracted by ammonium oxalate (Fe_o) relating to iron oxide pedogenetical low crystallinity the methodology of Schwertmann (1964).

Diffuse reflectance spectroscopy - hematite and goethite contents

Mineralogical attributes were estimated from the diffuse reflectance spectroscopy (DRS) of air-dried fine soil (ADFS) samples (particle diameter < 2.0 mm) (Torrent and Barrón, 2008). To this end, an amount of 1 g of soil was ground to uniform colour in an agate mortar and placed in the specimen holder with 16 mm diameter cylindrical space. Reflectance spectra were obtained with a spectrophotometer UV/Vis/NIR furnished with an integrating sphere 150 mm in diameter. Spectra were acquired at 0.5 nm intervals over the 380-780 nm range (i.e. in the visible region). The DRS technique yields a hematite:goethite ratio whereby their contents are estimated using mathematical calculations. The methodology used is described in greater detail elsewhere (Torrent and Barrón, 2008).

The contents of Hm and Gt were estimated from the second derivative of the Kubelka-Munk function (Yang and Kruse, 2004) for the DRS data according to

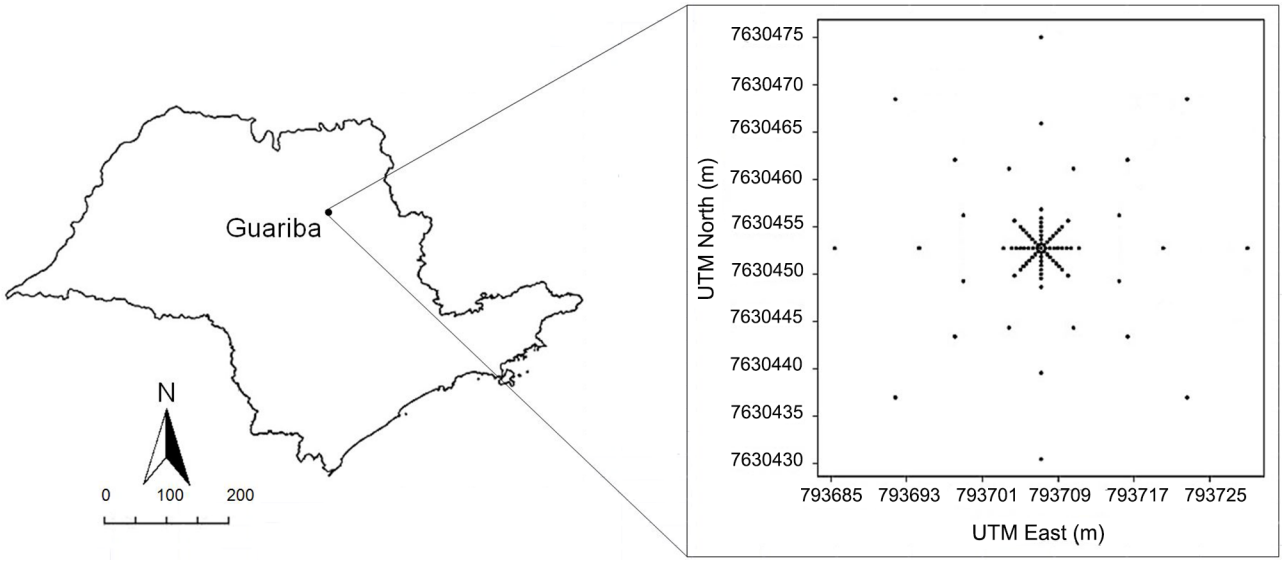

Figure 1 – Schematic depiction of the study area showing the location of the 89 points on the sampling grid.

Kosmas et al. (1984) and Scheinost et al. (1998):

$$f(R) = \frac{(1-R)^2}{2R} \quad (1)$$

where R is the sample diffuse reflectance. For this, an algorithm "smoothing" process was applied to adjust the "cubic spline" curve for the 31 reflectance value series (Scheinost et al., 1998). Thereafter, amplitudes of the spectral bands associated with the minerals Gt and Hm were determined according to Scheinost and Schwertmann (1999). For goethite detection 415-425 nm minimum and 440-450 nm maximum intervals were used, and for hematite: a minimum of 530-545 nm and maximum of 575-590 nm. Next the R parameter was obtained from the amplitude value (distance between the minimum and maximum values - Figure 2) of goethite and hematite absorption spectra:

$$R = \frac{A_{Hm}}{(A_{Hm} + A_{Gt})} \quad (2)$$

where: A_{Hm} is the amplitude of the band of hematite and A_{Gt} the amplitude band of goethite.

The ratio hematite/(hematite + goethite) ($Hm/(Hm + Gt)$) was estimated from the K factor as:

$$\begin{cases} K = -0.134 + 3.016R - 2.622R^2; if\ R < 0.6 \\ K = 0.40 + 0.60R; if\ R > 0.6 \end{cases} \quad (3)$$

The proportion of hematite (Hm) was calculated from the K factor as:

$$Hm = \frac{2.274\,(Fe_d - Fe_o)}{1.59 + 1.43\left(\frac{1-K}{K}\right)} \quad (4)$$

where: Fe_d is the iron extracted by sodium dithionite-citrate-bicarbonate and Fe_o is the iron extracted with oxalate.

The proportion of goethite (Gt) was calculated by the following equation:

$$Gt = 1.59\left[Fe_d - Fe_o - \left(\frac{Hm}{1.43}\right)\right] \quad (5)$$

As suggested by Scheinost et al. (1998), the bands in the spectral regions related to Gt and Hm were correlated with the contents in the two minerals as determined by X-ray diffraction. Soil samples can be analysed by DRS untreated because soil properties are not altered by any type of pre-treatment (Kosmas et al., 1984).

Statistical and geostatistical analysis

The attributes were preliminarily subjected to exploratory data analysis to calculate means, standard errors, standard deviations, coefficients of variation, minimum, maximum, asymmetry and kurtosis coefficients, and to check the normality hypothesis. The spatial variability of the target soil attributes was characterized by geostatistical analysis (Webster and Oliver, 1990), using the principles behind the intrinsic hypothesis, and simple and cross-semivariograms for modelling. The semivariance estimation at a given separation distance h, was determined by the following expression:

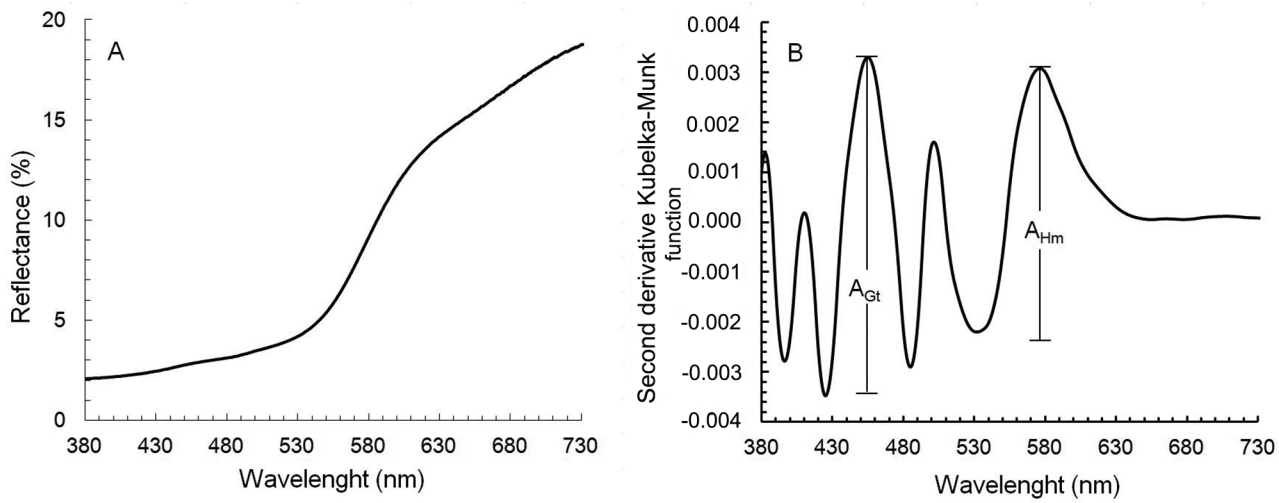

Figure 2 – Diffuse reflectance spectrum (A) and second derivative of the Kubelka–Munk function (B). Amplitudes of the spectral bandwidths assigned to goethite (A_{Gt}) and hematite (A_{Hm}) are shown.

$$\hat{\gamma}(h) = \frac{1}{2N(h)} \sum_{i=1}^{N(h)} [z(x_i) - z(x_i + h)]^2 \quad (6)$$

where: $\hat{\gamma}$ (h) is the experimental semivariance at h, $z(x_i)$ the value of the target property at point i, $N(h)$ the number of point pairs a distance h apart, $z(x_i)$ the value of z at point x_i and $z(x_i + h)$ at point $x_i + h$. The semivariogram describes the spatial continuity or dispersion of the variables as a function of the distances between locations.

Cross-semivariograms were modelled to characterize the spatial dependence between the main variables (FCO_2 and FWP) and an auxiliary or secondary variable (Hm, Gt or Fe_d). The semivariograms fitted the following equation:

$$\hat{\gamma}_{zy}(h) = \frac{1}{2N(h)} \sum_{i=1}^{N(h)} [z(x_i) - z(x_i + h)][y(x_i) - y(x_i + h)] \quad (7)$$

where: $\hat{\gamma}_{zy}(h)$ is the experimental cross-semivariance at an h distance; $z(x_i)$, main variable value estimated at i point; $y(x_i)$, secondary variable value at point i; and $N(h)$, the number of pairs of values separated by an h distance. The semivariogram originated from a special type of cross-semivariogram where semivariance is calculated for a single property and hence a spatial autocorrelation measurement for the concerned variable. Only those points where both the main variable and the secondary variable were simultaneously sampled were used to construct the cross-semivariogram.

Linear, Exponential, Gaussian and Spherical models were tested. The choice of the adjusted semivariogram model was based on the coefficient of determination (R^2), obtained by fitting the theoretical model to the experimental semivariograms and in cross-validation. Cross-validation was based on root mean square error (RMSE) (Equation 8) and mean error (ME) (Equation 9) (Cerri et al., 2004; Chirico et al., 2007); the lower the RMSE and ME, the higher the accuracy and the lower the bias in the estimates, respectively.

$$RMSE = \left\{ \frac{1}{n} \sum_{i=1}^{n} \left[z(x_i) - \hat{z}(x_i) \right]^2 \right\}^{0,5} \quad (8)$$

$$ME = \frac{1}{n} \sum_{i=1}^{n} \left[z(x_i) - \hat{z}(x_i) \right] \quad (9)$$

where n is the number of values used for validation, $z(x_i)$ the value of the property concerned at point i and $\hat{z}(x_i)$ its estimated counterpart. The RMSE provides information on model accuracy for each variable and the ME assesses its trend.

Models regressions were developed to predict FCO_2 and FWP from the Hm, Gt and Fe_d contents. In our study, we separated about 10 % of the total of 89 data points for external validation, and the remaining 90 % were used for modelling (Cerri et al., 2004; Chirico et al., 2007). External validation provides the opportunity to compare observed and estimated data. External validation analysis was assessed based on the RMSE (eq. 8) and ME (eq. 9), which evaluate accuracy and bias of the models, respectively (Cerri et al., 2004; Chirico et al., 2007).

The estimates of the semivariogram models were obtained using the GS+ software (version 9.0; Gamma Design Software, LLC, Plainwell, MI, USA). Descriptive statistics were performed using the SAS software (Statistical Analysis System, Institute, Cary, NC, USA, version 9.0).

Results and Discussion

The mean FCO_2 (2.19 μmol m^{-2} s^{-1}) and its coefficient of variation (CV = 37 %), Table 1, were similar to those previously reported for similar crops and soils (Brito et al., 2010; Panosso et al., 2009; Panosso et al., 2012). The coefficient of variation is a measure of variability in soil attributes. Based on the classification of Warrick and Nielsen (1980), Hm and Fe_d had a moderate coefficient (12 % < CV < 24 %), and FCO_2, FWP and Gt had a high coefficient (CV > 24 %). A number of attributes exhibited rather broad variability for the small sampling area used.

The high CV value for FCO_2, 37 %, is typical of this attribute as has been previously reported for a variety of soils and crop types (La Scala et al., 2000; Herbst et al., 2012). Panosso et al. (2012), who studied the fractal dimension and anisotropy of soil respiration in a mechanically harvested sugarcane area, observed spatial variability of soil CO_2 emission was predominantly explained by changes in the oxygen level of the soil, as expressed by FWP. Therefore, the high CV values obtained for these two properties suggest that FCO_2 and FWP have similar variability.

FCO_2, Hm and Fe_d exhibited a non-normal distribution (Anderson-Darling test; $p < 0.01$; Table 1). Although this is not required for data used in geostatistical analysis, we opted to convert FCO_2, Hm and Fe_d data to logarithmic form prior to variographic analysis, which is a common practice in spatial analyses (Kosugi et al., 2007; Panosso et al., 2009). The theoretical distribution of data from a natural source can only be fitted in an approximate manner, so the data need not be normalized for geostatistical analysis provided the distribution is not exceedingly asymmetric (Cressie, 1991).

The spatial correlation between mineralogical attributes, FCO_2 and FWP was elucidated by using simple and cross-semivariograms (Table 2, Figures 3 and 4). All attributes exhibited spatial dependence that was elucidated by fitting the semivariograms. The spherical mod-

Table 1 – Mean, standard deviation, minimum and maximum value, and coefficient of variation of the target soil attributes as measured in the 0.00-0.10 m soil layer at 89 sampling points.

Attribute	Mean	ME	SD	CV (%)	Min.	Max.	CA	Kurt.	AD (*p*)
FCO_2 (μmol m^{-2} s^{-1})	2.19	0.09	0.81	36.7	0.79	4.87	0.72	0.56	< 0.01
FWP (%)	15.42	0.66	5.72	38.1	1.81	27.03	-0.65	0.75	0.13
Hm (g kg^{-1})	103.15	1.95	17.60	17.1	47.40	133.58	-0.74	-0.02	< 0.01
Gt (g kg^{-1})	42.17	1.90	10.35	24.5	18.11	113.81	-0.45	0.11	0.11
Fe_d (g kg^{-1})	105.64	1.20	17.08	16.2	48.94	129.59	-0.81	-0.07	< 0.01

N = 89. FCO_2 = Soil CO_2 emission, FWP = free water porosity; Hm = hematite content; Gt = goethite content; Fe_d = iron extracted by sodium dithionite-citrate-bicarbonate; ME = standard error of the mean; SD = standard deviation; CV = coefficient of variation; Min. = minimum value; Max. = maximum value; CA = coefficient of asymmetry; Kurt. = kurtosis; AD = Anderson–Darling normality test.

Table 2 – Model type and parameters of the simple and cross-semivariograms fitted to the FCO_2, FWP, Hm, Gt and Fe_d values.

Parameter	Model	C_0	$C_0 + C_1$	$C_0/(C_0+C_1)$	Range (m)	R^2	RMSE	ME
FCO_2	Sph.	0.24	0.57	0.42	3.90	0.97	0.09	-0.03
FWP	Sph.	11.34	25.15	0.45	3.24	0.93	0.51	0.27
Hm	Exp.	45.00	257.08	0.17	1.60	0.96	1.53	-0.13
Gt	Sph.	24.64	53.67	0.46	1.90	0.90	0.75	-0.28
Fe_d	Sph.	114.15	259.20	0.44	2.22	0.87	1.37	-0.18
FCO_2 × Hm	Sph.	1.30	5.15	0.25	2.58	0.86	-	-
FCO_2 × Gt	Sph.	0.15	2.21	0.07	2.92	0.95	-	-
FCO_2 × Fe_d	Sph.	0.97	5.99	0.16	3.14	0.95	-	-
FWP × Hm	Sph.	1.45	37.55	0.04	3.26	0.97	-	-
FWP × Gt	Sph.	2.01	16.25	0.12	3.60	0.92	-	-
FWP × Fe_d	Sph.	3.05	34.41	0.09	3.50	0.85	-	-

FCO_2 = Soil CO_2 emission; FWP = free water porosity; Hm = hematite content; Gt = goethite content; Fe_d = iron extracted by sodium dithionite-citrate-bicarbonate; C_0 = nugget effect; $C_0 + C_1$ = sill; $C_0/(C_0 + C_1)$ = degree of spatial dependence; RMSE = root mean square error; ME = mean error; Sph. = spherical; Exp. = exponential.

el was adjusted to the simple and cross-semivariograms for all attributes except Hm content. The exponential model provides a better description of an Hm simple semivariogram. The spherical model is suitable for most soil attributes (Cambardella et al., 1994). The asymptotic sill of the exponential model is responsible for mild transitions in space, which are typical of attributes changing abruptly in the field. Camargo et al. (2014) applied spherical, exponential and gaussian models to a soil of the same type. Additionally, La Scala et al. (2000), Brito et al. (2010) and Panosso et al. (2009) have used spherical models to fit CO_2 emission semivariograms on the same soil type and crop.

Based on the classification of Cambardella et al. (1994), our FCO_2, FWP, Gt and Fe_d simple semivariograms exhibited moderate spatial dependence, with $0.25 < C_0/(C_0 + C_1) < 0.75$. On the other hand, the simple semivariogram for Hm and all of its cross-semivariograms exhibited marked spatial dependence, with $C_0/(C_0 + C_1) < 0.25$ - which testifies to the strong spatial correlation between the mineralogical attributes, FCO_2 and FWP.

The range distance for FCO_2 (3.90 m) was smaller than that reported by Brito et al. (2010), who examined soil respiration at three different topographic locations containing a 69-point, 90 m × 90 m sampling grid each. However, our results are similar to those of Kosugi et al. (2007) for forest areas; they detected bands of 4.40-27.70 m in a 50 m × 50 m sampling grid. La Scala et al. (2000) studied temporal changes in FCO_2 spatial variability in bare soil and obtained range distance values from 29.60 to 58.40 m.

The accuracy of the estimates provided by the simple semivariograms for each variable was assessed in terms of RMSE and ME (Table 2). The variables FCO_2 and FWP accounted for more than 50 % of the variability at the points used for cross-validation (RMSE < 0.71) (Hengl, 2007). FWP was slightly overestimated (ME = 0.27), whereas all other variables were underestimated (ME < 0) - particularly Gt, with ME = -0.28. Based on the results, the spatial modelling methodology used provides estimates that are very close to the measured values and is, therefore, an effective predictor of soil attributes.

There were positive correlations between soil respiration and the mineralogical attributes Hm ($r = 0.64$, $p < 0.01$) and Gt ($r = 0.65$, $p < 0.01$) (Figure 5A, B). La Scala et al. (2000) studied spatial variability in soil respiration in the same region and obtained significant correlations between FCO_2 and the amounts of organic carbon and iron extracted from clays, which are closely related to the spectral reflectance of soil (Demattê et al., 2006; Viscarra Rossel and Webster, 2011). The positive correlations between Hm, Gt and FCO_2 may have resulted from the favorable effect of iron oxides on soil respiration (La Scala et al., 2000); in fact, these clay minerals influence aggregation of soil particles (Duiker et al., 2003; Cañasveras et al., 2010) and, together with moisture, govern CO_2 release from the soil into the atmosphere (Nazaroff, 1992). There-

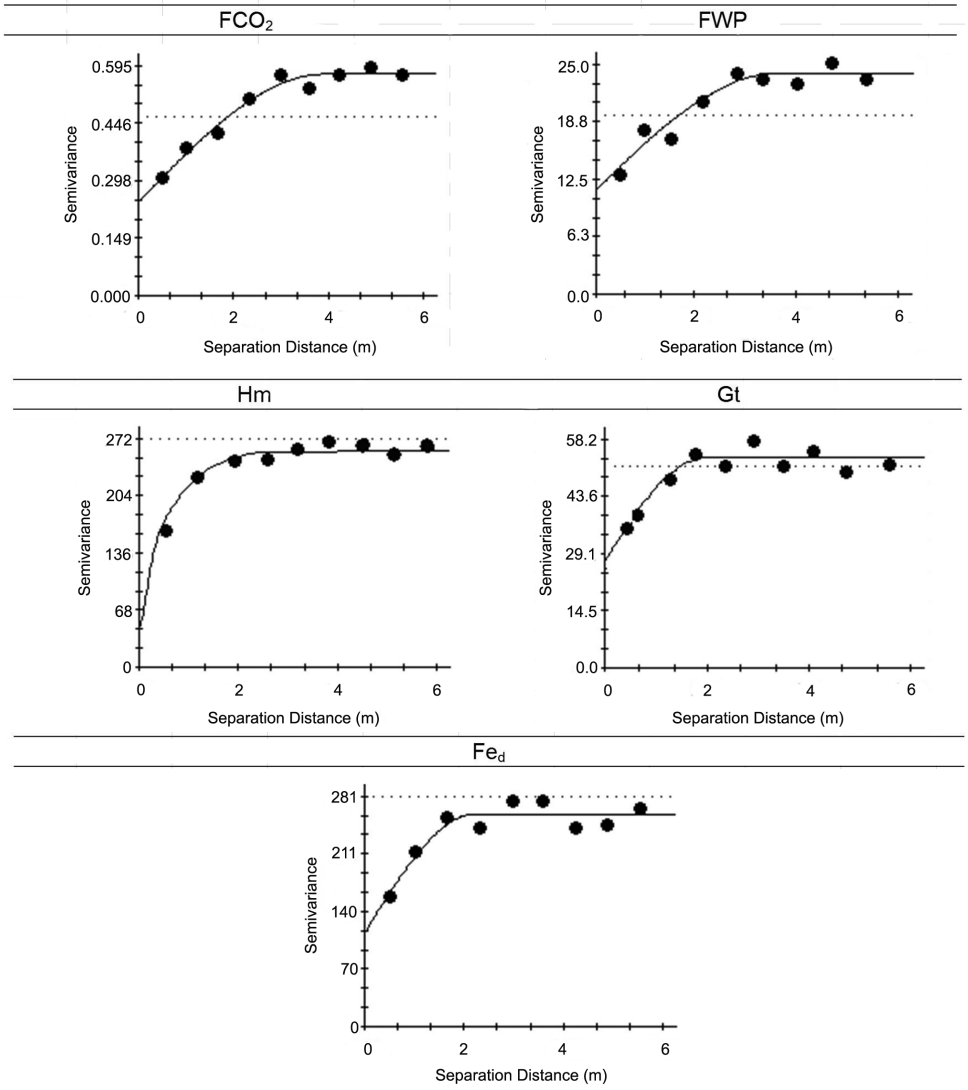

Figure 3 – Simple semivariograms fitted to soil CO_2 emission (FCO_2), free water porosity (FWP), hematite (Hm), goethite (Gt) and iron extracted by sodium dithionite-citrate-bicarbonate (Fe_d).

fore, FCO_2 must also be correlated with Fe_d, which is a structural component of these clay minerals (Figure 5C). Cañasveras et al. (2010) used DRS to estimate stability indices for Mediterranean soil aggregates and found iron oxides, as well as the contents in clay, calcium carbonate and organic matter, among other soil properties, to influence them. We found a positive correlation ($r = 0.64$, $p < 0.01$) between Fe_d and FCO_2, which is suggestive of a direct proportionality between the two parameters and contradicts previous results of La Scala et al. (2000) for soil respiration in a bare Oxisol. These authors obtained negative linear correlation coefficients of -0.22, -0.36 and -0.42, respectively, between Fe_d and FCO_2 on three different dates.

La Scala et al. (2000) and Bahia et al. (2014) suggest more complex relationships between minerals in clay fraction and biological activity in soil. Inda et al. (2007) studied tropical and subtropical soils and found that stability of organomineral complexes was directly related to organic matter content and clay fraction mineralogy. In addition to these factors, the iron content of soil is judged important to the assessment of the impact of preparation and management practices in tropical soils (La Scala et al., 2000). Therefore, elucidating iron contents and CO_2 losses in Brazilian soils implies using additional techniques (especially DRS) due to the high variability.

Free water porosity (FWP) was positively correlated with Hm ($r = 0.65$, $p < 0.01$), Gt ($r = 0.62$, $p < 0.01$) and Fe_d ($r = 0.69$, $p < 0.01$) (Figure 5D, E, F). Again, this may have resulted from the effect of mineralogical attributes (particularly iron oxides) on

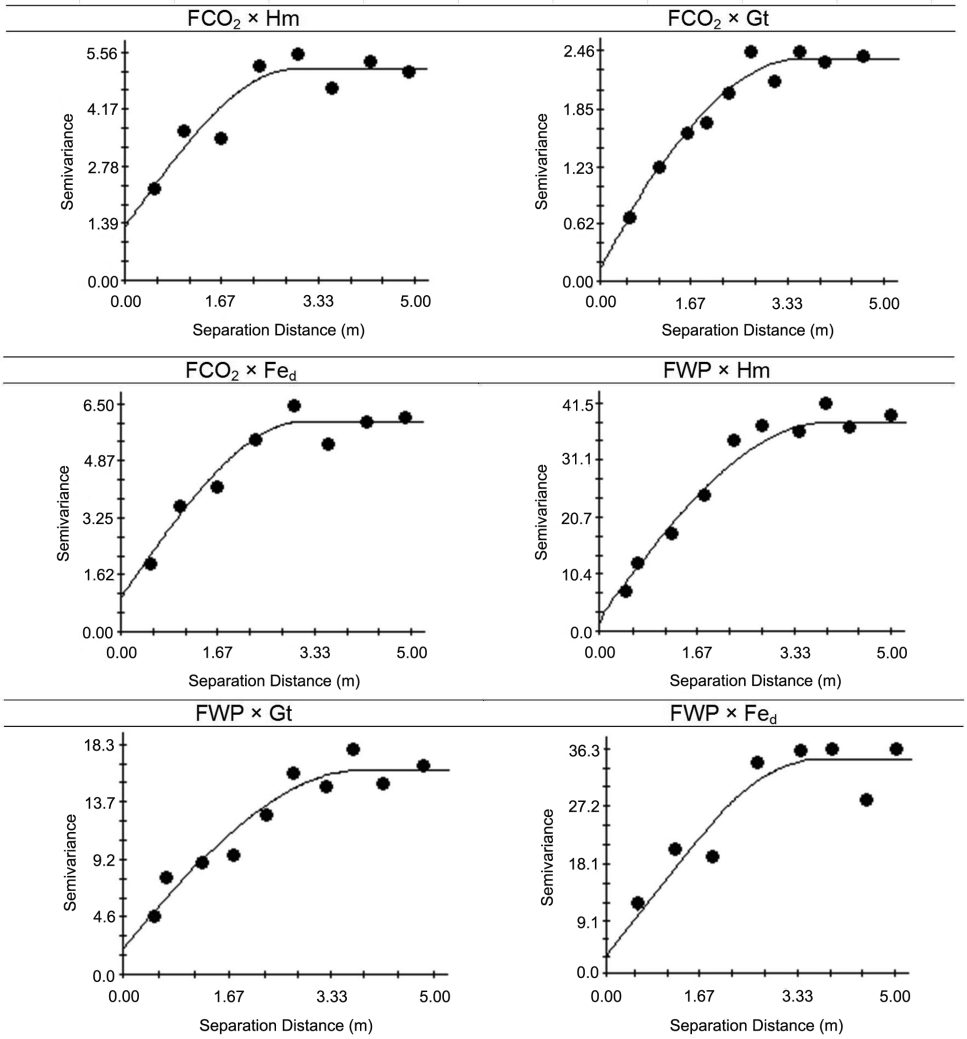

Figure 4 – Cross-semivariograms fitted to soil CO_2 emission (FCO_2), free water porosity (FWP), hematite (Hm), goethite (Gt) and iron extracted by the sodium dithionite-citrate-bicarbonate (Fe_d).

soil aggregation (Duiker et al., 2003; Cañasveras et al., 2010). Soil aggregation results from the complexing of clay particles by organic matter and multivalent metals such as iron; the organic constituents act as ligands and occupy the central portion of the aggregates, thereby increasing their stability (Tisdall and Oades, 1982). One can therefore expect that FCO_2 is directly related to clay mineral content in such a way that the greater the bonding agent amount in soil, the lower the water content and the easier it will be for CO_2 to be released into the atmosphere as in Fick's law (Ghildyal and Tripathi, 1987; Nazaroff, 1992). Respiration in bare soils comes directly from microbial activity, which is influenced by the presence of iron oxides as constituents of clay materials.

The goethite content exhibited the highest linear correlation (Figure 5B) and also the highest spatial correlation, especially with FCO_2 (Table 2), with a nugget effect C_0 = 0.15 and a degree of spatial dependence $C_0/(C_0 + C_1)$ = 0.07. Such results testify to the usefulness of mineralogical information (particularly the content in Gt) for the spatial characterization of FCO_2. As observed for simple linear correlation (Figure 5), all attributes presented positive spatial correlation, generating positive nugget effect (C_0) and range ($C_0 + C_1$) (Figure 3). Stoyan et al. (2000) previously found positive spatial correlations between FCO_2, soil moisture and carbon content in forest areas. Camargo et al. (2008) studied an Oxisol on various forms of relief and observed spatial correlation between mineralogical attributes and soil aggregates. This result confirms the hypothesis that soil oxygenation is related to microaggregation since the iron oxides Hm and Gt are constituents of the clay fraction and can thus affect soil CO_2 emission.

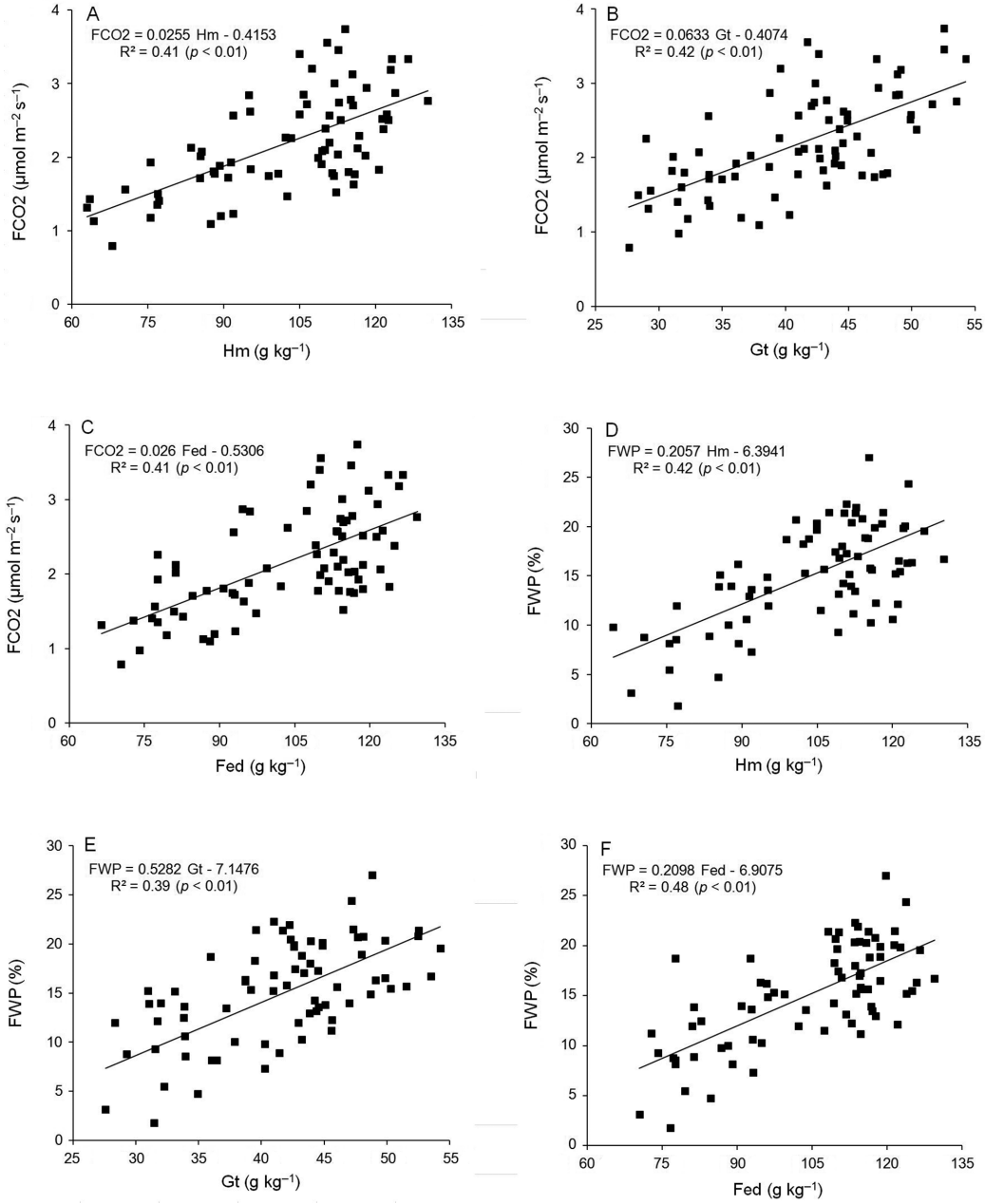

Figure 5 – Linear regression models for the observed data of soil CO_2 emission (FCO_2) with hematite (Hm) (A), goethite (Gt) (B) and iron extracted by sodium dithionite-citrate-bicarbonate (Fe_d) (C) and free water porosity (FWP) with Hm (D), Gt (E) and Fe_d (F).

The prediction capacity of regression models was determined using external validation as it provides an opportunity to compare observed and estimated data. Regression coefficients between observed values of FCO_2 (using reference method, field-measurement) and predicted values (DRS-estimated) were 0.96; 0.96; and 0.89 for Hm; Gt; and Fe_d, respectively. In the case of FWP, coefficients were 0.96; 0.91; and 0.92 for Hm; Gt; and Fe_d, respectively (Table 3); estimate quality was assessed by accuracy indexes (RMSE and ME). According to Hengl (2007), RMSE values below 0.71 indicate that the model concerned accounts for more than 50 % of the variability at the points used for external validation. One other fact that should be considered is the low ME values obtained, that is an indicator of bias model in the estimative, i.e. assesses the trend on model (Hengl, 2007). According to the ME values, the estimates for the FCO_2 using Hm (0.08) and Fed (-0.06) as predictor variables were those exhibiting the least bias, whereas for the FWP estimatives, Hm (0.08) and Gt (-0.06) exhibited smaller bias. The Gt was

Table 3 – Accuracy-related parameters of external validation of soil CO_2 emission (FCO_2) and free water porosity (FWP) as estimated by the regression models.

	r	RMSE	ME	AD (*p*)
FCO2				
$FCO2_{Hm}$	0.96**	0.24	0.08	0.211
$FCO2_{Gt}$	0.96**	0.29	-0.26	0.207
$FCO2_{Fed}$	0.89**	0.34	-0.06	0.127
FWP				
FWP_{Hm}	0.96**	0.28	0.08	0.914
FWP_{Gt}	0.91**	0.56	-0.06	0.200
FWP_{Fed}	0.92**	0.39	0.16	0.089

(n = 9); **significant as $p < 0.01$. FCO_2 = Soil CO_2 emission, FWP = free water porosity; Hm = hematite content; Gt = goethite content; Fe_d = iron extracted by sodium dithionite-citrate-bicarbonate; *r* = Pearson correlation coefficients; RMSE = root mean square error; ME = mean error; AD = Anderson-Darling normality test applied to the equation residuals.

the predictor variable with the greatest data underestimation for FCO_2, with an ME value of -0.26.

Certainly, direct measurements of the properties are more accurate than predictions generated from mathematical models. However, conventional laboratory analyses are expensive and require a long time. So, the DRS technique provides an effective choice for this purpose as it allows for easy identification and estimation of soil attributes, including the attributes involved in soil respiration (e.g. Hm, Gt and Fe_d). Diffuse reflectance spectroscopy is thus a promising tool in spatial variability studies of FCO_2 and FWP that are closely related to spatial variability in soil respiration (Panosso et al., 2012; Bahia et al., 2014).

The accuracy of the proposed models is well spent in tropical regions in the same range of iron oxide concentrations with the same cropping system as we use a on a small-spatial scale. However, we believe that this method is also suitable for other conditions, such as tropical soil types, iron oxide content, sampling scale, and crop history which, however, require prediction model adjustments. In this way, the technique can be a useful tool for precision agriculture once it assists CO_2 emission and free water porosity mapping for large areas. Thus, our results will contribute to elaborate greenhouse gas emission inventories in agricultural soils, collaborating with global climate change studies as far as the soil CO_2 emission remains one of the major sources of carbon release into the atmosphere.

Conclusions

Contents in hematite, goethite and sodium dithionite-citrate-bicarbonate iron were positively correlated with field-measured soil CO_2 emission and free water porosity. All studied attributes and their interactions exhibited spatial dependence structure, which was elucidated by modelling the spherical and exponential semivariograms. Using geostatistical techniques facilitated interpretation of the spatial relationships between soil respiration and the soil properties examined.

Acknowledgement

To the Graduate Program in Plant Production, UNESP/Jaboticabal for master degree fellowship to the first author; for the São Paulo State Foundation for Research Support (FAPESP) and the Brazilian National Council for Scientific and Technological Development (CNPq) for the financial support.

References

Bahia, A.S.R.S.; Marques Jr., J.; Panosso, A.R.; Camargo, L.A.; Siqueira, D.S.; La Scala, N. 2014. Iron oxides as proxies for characterizing anisotropy in soil CO_2 emission in sugarcane areas under green harvest. Agriculture, Ecosystems Environment 192: 152-162.

Brito, L.F.; Marques Jr., J.; Pereira, G.T.; La Scala, N. 2010. Spatial variability of soil CO_2 emission in different topographic positions. Bragantia 69: 19-27.

Camargo, L.A.; Marques Jr., J.; Pereira, G.T.; Bahia, A.S.R.S. 2014. Clay mineralogy and magnetic susceptibility of Oxisols from Bauru Group Sandstones in different geomorphic surfaces. Scientia Agricola 71: 244-256.

Camargo, L.A.; Marques Jr., J.; Pereira, G.T.; Horvat, R.A. 2008. Spatial variability of mineralogical attributes of an Oxisol under different relief forms. I. Clay fraction mineralogy. Revista Brasileira de Ciência do Solo 32: 2269-2277 (in Portuguese, with abstract in English).

Cambardella, C.A.; Moorman, T.B.; Novak, J.M.; Parkin, T.B.; Karlen, D.L.; Turco, R.F.; Konopka, A.E. 1994. Field-scale variability of soil properties in central Iowa soils. Soil Science Society America Journal 58: 1501-1511.

Cañasveras, J.C.; Barrón, V.; Del Campillo, M.C.; Torrent, J.; Gómez, J.A. 2010. Estimation of aggregate stability indices in Mediterranean soils by diffuse reflectance spectroscopy. Geoderma 158: 78-84.

Cerri, C.C.; Maia, S.M.F.; Galdos, M.V.; Cerri, C.E.P.; Feigl, B.J.; Bernoux, M. 2009. Brazilian greenhouse gas emissions: the importance of agriculture and livestock. Scientia Agricola 66: 831-843.

Cerri, C.E.P.; Bernoux, M.; Volkoff, B.; Victoria, R.L.; Melillo, J.M.; Paustian, K.; Cerri, C.C. 2004. Assessment of soil property spatial variation in an Amazon pasture: basis for selecting an agronomic experimental area. Geoderma 123: 51-68.

Chirico, G.B.; Medina, H.; Romano, N. 2007. Uncertainty in predicting soil hydraulic properties at the hillslope scale with indirect methods. Journal of Hydrology 334: 405-422.

Cornell, R.M.; Schwertmann, U. 2003. The Iron Oxides: Structure, Properties, Reactions, Occurrence and Uses. VCH Publishers, Weinheim, Germany.

Cressie, N. 1991. Statistics for spatial data. John Wiley, New York, NY, USA.

Demattê, J.A.M.; Sousa, A.A.; Alves, M.C.; Nanni, M.R.; Fiorio, P.R.; Campos, R.C. 2006. Determining soil water status and other soil characteristics by spectral proximal sensing. Geoderma 135: 179-195.

Duiker, S.W.; Rhoton, F.E.; Torrent, J.; Smeck, N.E.; Lal, R. 2003. Iron (hydr)oxide crystallinity effects on soil aggregation. Soil Science Society of America Journal 66: 606-611.

Ghildyal, B.P.; Tripathi, R.P. 1987. Soil Physics. John Wiley, New York, NY, USA.

Hengl, T.A. 2007. Practical Guide to Geostatistical Mapping of Environmental Variables. European Commission-JRC, Ispra, Italy. (JRC Scientific and Technical Reports).

Herbst, M.; Bornemann, L.; Graf, A. 2012. A geostatistical approach to the field-scale pattern of heterotrophic soil CO_2 emission using covariates. Biogeochemistry 111: 377-392.

Inda, A.V.; Bayer, C.; Conceição, P.C.; Boeni, M.; Salton, J.C.; Tonin, A.T. 2007. Selected soil-variables related to the stability of organo-minerals complexes in tropical and subtropical Brazilian soils. Ciência Rural 37: 1301-1307 (in Portuguese, with abstract in English).

Inda, A.V.; Torrent, J.; Barrón, V.; Bayer, C.; Fink, J.R. 2013. Iron oxides dynamics in a subtropical Brazilian Paleudult under long-term no-tillage management. Scientia Agricola 70: 48-54.

Kosmas, C.S.; Curi, N.; Bryant, R.B. 1984. Characterization of iron oxide minerals by second-derivative visible spectroscopy. Soil Science Society of America Journal 48: 401-405.

Kosugi, Y.; Mitani, T.; Ltoh, M.; Noguchi, S.; Tani, M.; Matsuo, N.; Takanashi, S.; Ohkubo, S.; Nik, A.R.; 2007. Spatial and temporal variation in soil respiration in a Southeast Asian tropical rainforest. Agricultural and Forest Meteorology 147: 35-47.

La Scala, N.; Marques Jr., J.; Pereira, G.T.; Corá, J.E. 2000. Carbon dioxide emission related to chemical properties of a tropical bare soil. Soil Biology and Biochemistry 32: 1469-1473.

Mehra, O.P.; Jackson, M.L. 1960. Iron oxide removal from soils and clays by a dithionite-citrate system buffered with sodium bicarbonate. Clays and Clay Minerals 7: 317-327.

Nazaroff, W.W. 1992. Radon transport from soil to air. Reviews of Geophysics 30: 137-160.

Panosso, A.R.; Marques Jr., J.; Pereira, G.T.; La Scala, N. 2009. Spatial and temporal variability of soil CO_2 emission in a sugarcane area under green and slash-and burn management. Soil Tillage Research 105: 275-282.

Panosso, A.R.; Perillo, L.I.; Ferraudo, A.S.; Pereira, G.T.; Miranda, J.G.V.; La Scala, N. 2012. Fractal dimension and anisotropy of soil CO_2 emission in a mechanically harvested sugarcane production area. Soil Tillage Research 124: 8-16.

Scheinost, A.C.; Chavernas, A.; Barrón, V.; Torrent, J. 1998. Use and limitations of second-derivative diffuse reflectance spectroscopy in the visible to near infrared range to identify and quantify Fe oxides in soils. Clays and Clay Minerals 46: 528-536.

Scheinost, A.C.; Schwertmann, U. 1999. Color identification of iron oxides and hydroxysulfates: use and limitations. Soil Science Society of American Journal 63: 1463-1471.

Schwertmann, U. 1964. Differentiation of iron oxides of the soil by extraction with ammonium oxalate solution = Differenzierung der Eisenoxide des Bodens durch Extraktion mit Ammoniumoxalat-Lösung. Zeitschrift für Pflanzenernährung, Düngung, Bodenkunde 105: 194-202 (in German).

Schwertmann, U.; Taylor, R.M. 1989. Iron oxides. p. 379-438. In: Dixon, J.B.; Weed, S.B., eds. Minerals in soil environments. 2ed. Soil Science Society of America, Madison, WI, USA.

Soil Survey Staff. 1999. Soil Taxonomy: A Basic System of Soil Classification for Making and Interpreting Soil Surveys. 2ed. USDA-NRCS, Washington, DC, USA.

Stoyan, H.; De-Polli, H.; Böhm, S.; Robertson, G.P.; Paul, E.A. 2000. Spatial heterogeneity of soil respiration and related properties at the plant scale. Plant and Soil 222: 203-214.

Tisdall, J.M.; Oades, J.M. 1982. Organic matter and water stable aggregates in soils. Journal of Soil Science 33: 141-163.

Torrent, J.; Barrón, V. 2008. Diffuse reflectance spectroscopy. p. 367-385. In: Ulery, A.L.; Drees, L.R., eds. Methods of soil analysis. Part 5. Mineralogical methods. Soil Science Society of America, Madison, WI, USA.

Viscarra Rossel, R.A.; Webster, R. 2011. Discrimination of Australian soil horizons and classes from their visible–near infrared spectra. European Journal of Soil Science 62: 637-647.

Warrick, A.W.; Nielsen, D.R. 1980. Spatial variability of soil physical properties in the field. p. 319-344. In: Hillel, D., ed. Applications of soil physics. Academic Press, New York, NY, USA.

Webster, R.; Oliver, M.A. 1990. Statistical Methods in Soil and Land Resource Survey. Oxford University Press, Oxford, UK.

Yang, L.; Kruse, B. 2004. Revised Kubelka-Munk theory. I. Theory and application. Journal of the Optical Society of America 21: 1933-1941.